

Size and shape based chromosome separation in the inertial focusing device

SCI F

Cite as: Biomicrofluidics 14, 064109 (2020); doi: 10.1063/5.0026281

Submitted: 23 August 2020 · Accepted: 23 October 2020 ·

Published Online: 2 December 2020



View Online



Export Citation



CrossMark

Haidong Feng,¹ Matthew Hockin,² Mario Capecchi,² Bruce Gale,¹ and Himanshu Sant^{1,a)}

AFFILIATIONS

¹ Department of Mechanical Engineering, University of Utah, Salt Lake City, Utah 84112, USA² Eccles Institute of Human Genetics, University of Utah, Salt Lake City, Utah 84112, USA^{a)} Author to whom correspondence should be addressed: himanshu.sant@utah.edu

ABSTRACT

In this paper, we use a spiral channel inertial focusing device for isolation and purification of chromosomes, which are highly asymmetric. The method developed is proposed as a sample preparation process for transchromosomal research. The proposed microfluidics-based chromosome separation approach enables rapid, label-free isolation of bioactive chromosomes and is compatible with chromosome buffer. As part of this work, particle force analysis during the separation process is performed utilizing mathematic models to estimate the expected behavior of chromosomes in the channel and the model validated with experiments employing fluorescent beads. The chromosome sample is further divided into subtypes utilizing fluorescent activated cell sorting, including small condensed chromosomes, single chromosomes, and groups of two chromosomes (four sister chromatids). The separation of chromosome subtypes is realized based on their shape differences in the spiral channel device under high flow rate conditions. When chromosomes become aligned in the shear flow, the balance between the inertial focusing force and the Dean flow drag force is determined by the chromosome projection area and aspect ratio, or shape difference, leading to different focusing locations in the channel. The achieved results indicate a new separation regime in inertial microfluidics that can be used for the separation of non-spherical particles based on particle aspect ratios, which could potentially be applied in fields such as bacteria subtype separation and chromosome karyotyping.

Published under license by AIP Publishing. <https://doi.org/10.1063/5.0026281>

I. INTRODUCTION

Advances in genetic technology have enabled the direct manipulation of entire chromosomes for chromosome transfer experiments,¹ which provide means for a better understanding of basic biology and the human genome. These transferred chromosomes could also be an ideal platform for the study of human disease and genetic expression.^{2–4} The isolation and purification of the chromosomes is an important step in the sample preparation process for these experiments. Chromosomes can be extracted from donor cells and transferred into recipient cells, typically while the chromosomes are condensed during metaphase. Metaphase chromosomes are assemblies of linear DNA up to ~250 000 000 bp (Mbp) in length. Overall, this DNA molecule (250 Mbp, ~8 cm length, ~12 Å radius) is condensed, stabilized, and shaped as a rod-like particle approximately 6 μm × 0.25 μm (length × radius) through its interaction with >200 proteins.⁵ The individual chromosome DNA content varies from ~70 to 250 Mbp in both human and mouse cells and is highly related to their condensed

length. The collection of human chromosomes can be represented as a family of rods ~2–8 μm in length with a ~0.25 μm radius.

Chromosome isolation and purification methods include centrifugation, mechanical filtration, and fluorescent activated cell sorting (FACS). However, all of these separation approaches have limitations when applied to chromosome sample preparation. The centrifugation approach requires high spinning speeds, leading to chromosome degradation and sample loss. Density gradient centrifugation leads to a large osmotic deviation, and the removal of density agents takes extra sample treatment process and time. Mechanical filtration suffers from the problem of sample loss and absorption on the membrane surface.⁶ FACS is not a suitable chromosome separation approach as the low throughput and dilution limit the sorting process in a sample.⁷ Besides, the FACS process has specific requirements for the buffer compatibility with electrostatic gating, which sometimes is a conflict with the requirement of maintaining chromosomes in a biologically relevant buffer.

Improvement in the chromosome isolation approach is needed for the rapid separation of biologically active chromosomes. In this paper, chromosome separation is performed utilizing an inertial focusing microfluidic separation device. The inertial focusing device enables rapid, label-free particle sorting that has high separation resolution and efficiency. It avoids the tedious operations in traditional treatment processes and reduces the operator skill requirement. Inertial focusing separation has been used to separate blood cells,⁸ circulating tumor cells (CTCs),⁹ and sperms.¹⁰

This paper reports the separation of metaphase cell lysate (a mixture of cell debris, chromosome, and nuclei) performed utilizing an inertial focusing spiral channel device. The eluates have a complex composition of chromosome subtypes and nuclei. Experimental results show that chromosomes have different inertial focusing behavior compared with spherical particles with equivalent dimensions. The influence of the inertial flow and the Dean flow on the chromosome subtype movement is studied. A mathematical model is proposed to analyze chromosome separation based on their shape differences. The chromosome separation experiment is performed using a spiral microchannel, and the collected sample is analyzed through FACS sorting. The influence of experiment parameters is explored and discussed in Secs. II–V.

II. THEORY

Inertial focusing is the phenomenon wherein a particle laterally migrates across flow streamlines to a stable equilibrium position due to the particle–fluid interaction. In a confined microchannel, the high flow rate leads to the generation of a shear lift force (F_L),^{11,12} which drives particles into focused streams. The magnitude of F_L is determined by the flow velocity, channel dimension, and particle size,¹³

$$F_L = \frac{C_{SG}\rho U_{max}^2 d^4}{D_h^2}, \quad (1)$$

where C_{SG} is the lift coefficient, ρ is the fluid density, U_{max} is the maximum flow velocity, D_h is hydraulic mean diameter, and d is particle diameter.

In a spiral channel device, the channel curvature induces a secondary Dean flow in the channel cross section. The existence of the Dean flow changes the particle equilibrium position in the channel cross section.^{14–18} Particles with different shapes and dimensions can be separated by adjusting the balance between the shear lift force and the Dean drag force F_D ,

$$F_D = 3\pi\mu U_{De}d, \quad (2)$$

where μ is fluid viscosity. U_{De} is the Dean velocity, which can be estimated as $U_{De} = 1.8 \times 10^{-4} De^{1.63}$.¹⁹ Here, De is the Dean number, which is a dimensionless number for the Dean flow characterization.

In a spiral channel device, both the magnitudes of F_L and F_D are affected by the particle size. An increase in particle diameter leads to an increase of F_L over F_D . Size-based spherical particle separation can be achieved utilizing the co-effect of the inertial flow and the Dean flow. In a separation regime called Dean flow

fractionation, the shear lift force dominates the large particle movement, and the Dean drag force dominates the small particle movement. Large particles focus toward the inner wall in the spiral channel, and small particles are carried by the Dean flow and move toward the channel outer wall.²⁰ In the inertial–Dean flow coupled separation regime, both small and large particles become focused due to the inertial flow. The final particle stream focusing position is affected by the particle size and channel curvature. The unique location of particle focusing streams leading to multiple outlets results in particle separation.^{14,17}

Chromosomes are non-spherical bioparticles, and the shape of the chromosome affects chromosome separation in many ways. The magnitude of the Dean force and the shear lift force is affected by the particle shape and orientation in the flow, and more detailed force analysis for chromosome-shaped particles is needed to understand whether they will focus and, if they do, to what location. Non-spherical particles exhibit different focusing positions compared with spherical particles in the inertial flow. In the shear flow, the non-spherical particle movement has been predicted by Jeffery orbits (rotational diameter), but it is also found that non-spherical particles with high particle aspect ratios tend to become aligned with flow streamlines in a shear flow.^{21–23} The self-aligned particle will focus toward the center of the channel under the inertial focusing effect due to the hydrodynamic interaction between the asymmetric particles and the confined flow.^{24,25} In this case, the shear stress is higher in the channel height direction since the channel height h has a dimension smaller than channel width w . Spherical particles will have focus positions close to the top and bottom wall, while the chromosome will focus to the channel mid-plane. The existence of the Dean flow in the spiral channel device will lead to the lateral migration of particle focused streams. The Dean flow vortices flow toward the channel outer sidewall in the channel mid-plane and flow toward the channel inner sidewall near the channel top/bottom walls. As a result, the chromosome that focuses to the channel mid-plane migrates toward the channel outer sidewall, while spherical particles have a focus position close to the channel inner sidewall [Fig. 1(b)].

During mitosis, condensed chromosomes have the shape of fibers. Chromosomes are divided into two arms by centromere. Based on the location of the centromere, chromosomes are classified as metacentric, sub-metacentric, acrocentric, and telocentric chromosomes. The diameter of chromosome decreases near the centromere. In this case, the chromosomes are modeled as rod-shaped particles with a short axis a and a long axis b [Fig. 1(a)]. Utilizing current chromosome buffer, chromosomes are condensed and is treated as a rigid particle. The particle aspect ratio $\gamma = b/a$ is defined to characterize the chromosome shape. It is expected that a rod-shaped chromosome will become aligned with the fluid flow direction and have focusing positions close to the channel outer sidewall [Fig. 1(b)]. Chromosomes with different aspect ratios could potentially be separated based on the change of the shear lift force and the Dean flow drag force ratio. The magnitude of F_L is determined by the shear gradient experienced by the chromosome. When the chromosome becomes aligned with the primary flow direction, the apparent chromosome dimension for F_L is determined by the projection area of chromosome front view $A = \pi a^2/4$. Equation (1) is modified for chromosome shear lift force F_{Lc}

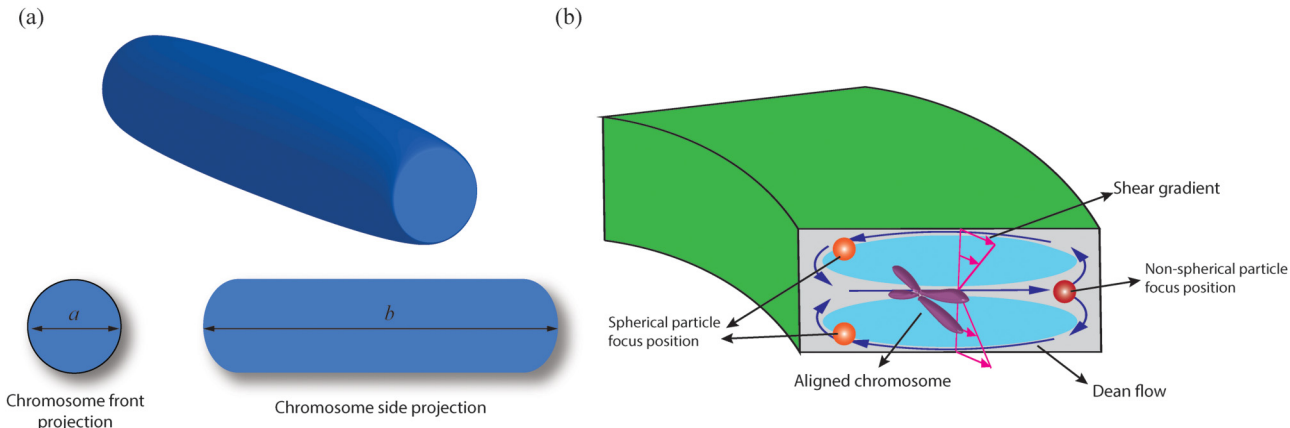


FIG. 1. (a) Demonstration of chromosome front and side projection area. (b) Diagram of chromosome alignment due to the inertial flow and the Dean flow.

calculation,

$$F_{Lc} = \frac{16C_{SG}\rho U_{max}^2 A^2}{\pi^2 D_h^2}. \quad (3)$$

The Dean drag force acts on the side or long direction of the chromosome, and the projection area is the side view of the capsule. The Dean flow drag force for chromosomes is estimated by a modified equation for chromosomes with aspect ratio γ^{26} as

$$F_{D\gamma} = 3\pi\mu U_{De} d_n K_n, \quad (4)$$

where d_n is the diameter of a sphere that has an equivalent projection area to the chromosome, K_n is the shape coefficient, $K_n = (d_n + 2d_s)/3d_m$, and d_s is the diameter of a sphere that has an equivalent surface area to the chromosome. With the increase of the chromosome aspect ratio, the Dean flow drag force will have a larger influence on the particle movement, leading to a change of particle focusing position. As a result, the separation of chromosomes based on the aspect ratio can be realized based on the co-effect of inertial focusing and the Dean flow in a spiral channel device.

In this model, we focused on the influence of chromosome aspect ratio and projection area on the chromosome movement. The influence of centromere is ignored to simplify the model. In the proposed model, the front projection area is affected by the maximum diameter in the chromosome cross section, and it does not change due to the existence of centromere structure. As a result, the chromosome aspect ratio is not affected in the rod-shape model. However, the rod-shape model induces a larger projection area in the side view compared with the actual chromosome. In some cases, the side projection area increases by 33%, leading to an increase of $F_{D\gamma}$ by 17%. Due to the variation of chromosome shape, it is hard to give an accurate prediction of chromosome movement trajectory in the fluid flow. In this paper, this model is used to

demonstrate the general movement trend of chromosome with different aspect ratios.

III. METHODOLOGY

A spiral channel device is proposed for the chromosome separation experiments. The channel cross section has a dimension of $150\text{ }\mu\text{m}$ in width and $50\text{ }\mu\text{m}$ in height. The channel curvature radius increases from 7.1 mm to 9.0 mm within four spiral loops. The analytical results indicate that the inertial focusing of $4\text{ }\mu\text{m}$ particles can be achieved with a proper flow rate and pressure drop (less than 340 KPa) in the current design. The spiral channel device design includes two inlet ports and four outlet ports marked as outlet 1–4 from the inner side channel to the outer side channel (Fig. 2).

The spiral channel device is made of polydimethylsiloxane (PDMS) and is fabricated utilizing photolithographically defined molds. The spiral channel device design is patterned on a chromium glass mask using a Heidelberg MicroPG 101 mask generator. Then, the pattern is transferred to a mold made with photoresist SU-8 3035 (Microchem, MA). The spiral channel height is determined by the photoresist thickness. PDMS (Sylgard 184, Dow Corning, MI) mixed with a curing agent is degassed and cast over the mold to form the spiral channel. The fabricated PDMS device is bonded with a glass slide using a corona treatment. Figure 2 (right) shows one of the spiral channel devices with two inlets and four outlets. The description of channel design can be found in the supplementary material.

Fluorescent polystyrene beads are used to observe particle focusing in the spiral channel device. $0.5\text{ }\mu\text{m}$ beads (Red color, Bangs Laboratories, IN) and $4.0\text{ }\mu\text{m}$ beads (Green color, Bangs Laboratories, IN) with particle concentration around 3×10^6 particles/ml are used. In the fluorescent bead separation experiments, particles are loaded from the inner or outer inlet, and the carrier solution is loaded from the other inlet. The flow rate is controlled using syringe pumps (KDS 230, KD Scientific, MA). One syringe pump pushes the sample into the spiral channel device, and

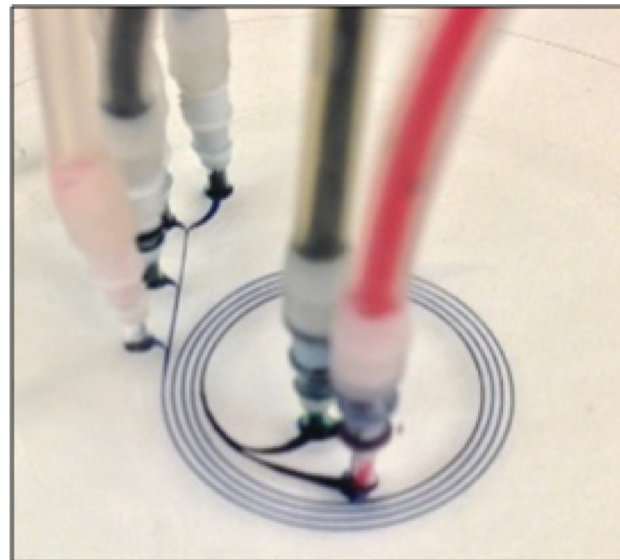
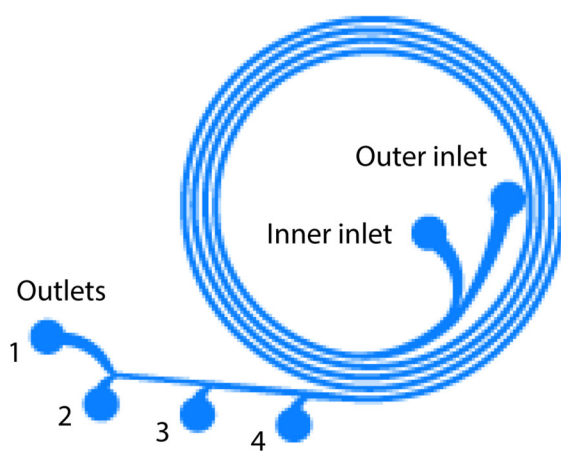


FIG. 2. Schematic diagram and image of the spiral microchannel device.

another pump pulls samples out of the spiral channel device through four outlets. The overall flow rate is changed from 0.05 ml/min to 0.8 ml/min. A fluorescent microscope is used to observe the focused particle streams. The particle stream is monitored at five different segments of the spiral channel device. The top segment is close to the device inlet region, and the bottom segment is close to the device outlet region. By identifying particle stream positions in the spiral channel, the particle and focusing separation performance is evaluated.

The chromosome sample is produced from metaphase mouse ES cells. A cell lysis process is performed utilizing a pinched flow microfluidic device,²⁷ and the cell lysate is composed of cell debris, DNA fractions, condensed chromosomes, clumps of chromosomes, and nuclei. The chromosome sample is suspended in the chromosome buffer that contains 70 mM KCl, 60 mM NaCl, 10 mM Hepes, and 1 mM EDTA. The solution pH is set to 7.2. Spermine, spermidine, adenylyl-imidodiphosphate (AMP-PNP), and a recombinant topoisomerase 2a (Top2a) fusion protein are added to the chromosome buffer prior to use, which contribute to the chromosome stability and condensation. Chromosome separation experiments follow the same experimental procedure as the fluorescent bead separation. When the sample is pushed through the spiral channel device, the eluate from four outlets is collected and analyzed. Collected samples are stained by Sytox green (Thermalfisher, MA), and fluorescent activated cell sorting (FACS) is performed to identify chromosome size and type.

IV. RESULTS

Fluorescent bead focusing and separation experiments were performed to examine the device performance. 4.0 μm beads were separated from 0.5 μm beads based on the Dean flow fractionation

mechanism. In the experiment, the large 4.0 μm beads were focused in the spiral channel due to the dominance of F_L , while the small 0.5 μm beads are dispersed and distributed due to the dominance of F_D . It was found that when the particle mixture was loaded in the outer side inlet with a total flow rate of 0.14 ml/min, large particles were focused to channel inner side, while small particles completed a full Dean circulation and exited the channel from the outer side outlets, which is referred to as Dean flow fractionation. In another case, particles were loaded in the inner inlet with a total flow rate of 0.08 ml/min. In this case, small particles completed half Dean loops and exited from the outer outlets. A detailed description of the fluorescent bead separation experimental results can be found in the [supplementary material](#).

The results of bead tests helped determine the best conditions for chromosome separation experiments. Accordingly, the first experiment for the separation of chromosomes and nuclei was performed using the Dean flow fractionation regime. The results of the FACS scan identifying the chromosome concentration after separation are shown in [Fig. 3](#). The different line colors indicate the material collected from the four outlets. In the first test, the sample is loaded from the inner side inlet with a flow rate of 0.08 ml/min. It is expected that the large chromosomes can be separated from small cell debris and chromosome pieces by these Dean flow fractionation conditions. The percent of chromosomes and nuclei in each outlet is 42.30%, 21.00%, 18.35%, and 18.35%. The results show that chromosomes do not have a tight focus stream in the spiral channel device, and they have a dispersed distribution in the channel outlet region. A control experiment was performed in which a sample was loaded from the outer side inlet at a flow rate of 0.08 ml/min [[Fig. 3\(b\)](#)]. The percentage of the chromosome in each outlet was 40.84%, 32.89%, 16.27%, and 10.0%. In this case, the Dean flow will deliver small particles from the outer side inlet

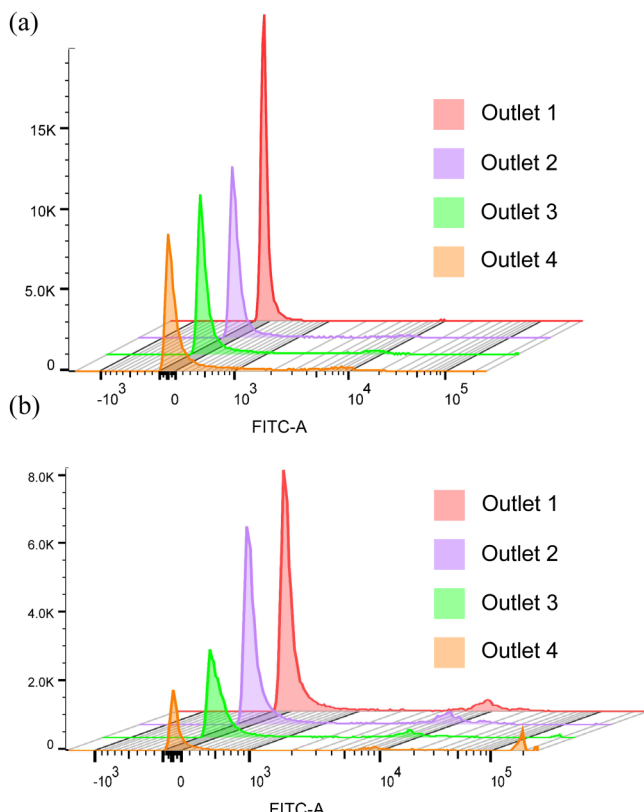


FIG. 3. FACS scans of chromosomes eluted from spiral channels. (a) The sample is loaded to the inside half of the channel. (b) The sample is loaded to the outside half of the channel.

toward the inner side outlet through the spiral channel device. As a result, the Dean flow contributes to the chromosome focusing toward the inner side outlets. However, the small-sized cell debris and DNA pieces are also carried by the Dean flow and migrate toward the inner channel outlets leading to a reduction of separation efficiency between the chromosomes and unwanted cell contents.

Experiments with high flow rates were performed to test chromosome focusing due to inertial effects. As an internal standard and to help guide the experiments, chromosome samples were loaded with $4.0\text{ }\mu\text{m}$ green fluorescent beads as well. Samples were loaded from the outer side inlet, and the flow rate was changed between 0.15 ml/min and 0.5 ml/min . Fractions from all four outlets were collected separately and analyzed using FACS. Figure 4 shows the plots obtained with the FACS analyzer. Inertial focusing of $4.0\text{ }\mu\text{m}$ beads was found at all test flow rates and the beads had sharp peaks in outlets 1 and 2 as shown in Fig. 4(a). The lateral movement of the $4.0\text{ }\mu\text{m}$ bead stream is observed with the increase of the flow rate. The peak moves gradually from outlet 4 toward outlet 3 as the flow rate increase to 0.5 ml/min . This phenomenon occurs due to the increased Dean flow with the increase of the flow rate, which will change the large particle focusing position.

Figure 4(b) shows the $0.5\text{ }\mu\text{m}$ bead distribution under different flow rates. The smaller beads were trapped in the Dean flow vortices and have different exit positions with the flow rate. At 0.15 ml/min , most of the beads moved to the outer sidewall region in the channel outlet area, while they moved toward the inner sidewall at 0.2 ml/min . The smaller beads had a higher concentration in the channel center at high flow rates. These results follow earlier data and confirm that our channel design and channel function is appropriate.

The chromosome sample had a distribution of 11%, 23%, 50%, and 16% in four outlets at a flow rate of 0.15 ml/min , and good separation of the chromosomes from $4\text{ }\mu\text{m}$ beads was achieved. The Dean flow fractionation effect appears to dominate the chromosome separation as the $0.5\text{ }\mu\text{m}$ beads have a similar distribution under the same flow rate [Fig. 4(b)]. With an increase in the flow rate, the chromosomes tend to be evenly distributed in the channel with a slight focus toward the middle of the channel. The comparison between chromosomes and $0.5\text{ }\mu\text{m}$ beads shows that the chromosomes behave very similar to $0.5\text{ }\mu\text{m}$ beads in the spiral channel device rather than the larger $4.0\text{ }\mu\text{m}$ beads.

The chromosome sample used in the test is a complex solution that contains different chromosome subtypes. The chromosome subtypes may behave differently in the spiral channel device and have different exit positions. The eluates from each of the four outlets are collected and analyzed using FACS sorting to help understand where the different subtypes may be eluting. The details of the FACS sorting process are provided in the [supplementary material](#). Four peaks are observed on the FACS histogram, which is used to isolate eluates into four fractions. Each of the fractions mainly composed: small condensed chromosomes (Fraction A), single chromosomes (Fraction B), groups of two chromosomes (Fraction C), and chromosome clumps/nuclei (Fraction D). Figure 5 shows the image of sorted chromosome subtypes and their distribution across the channel outlets. It is found that the small condensed chromosomes and single chromosomes have an even distribution in all outlets, and the increase of the flow rate does not affect their distribution. The groups of two chromosomes tend to focus on outlet 2 at a flow rate of 0.2 ml/min . The large chromosome clumps/nuclei tend to focus on the channel outer sidewall, and exit from outlet 1 at a flow rate of 0.2 ml/min .

V. DISCUSSION

The chromosome focusing experimental results indicate that improved purification of chromosomes can be achieved using the spiral channel device. However, the chromosome focusing phenomenon is different from both the $0.5\text{ }\mu\text{m}$ and $4.0\text{ }\mu\text{m}$ beads. It is found that the Dean flow has a higher influence on chromosome movement than the theoretical prediction, and new chromosome focusing positions are found in the spiral channel device. The chromosome sample used in the experiments consists of metaphase cell lysates, which is a complex system, including chromosomes, small DNA pieces, cell debris, and other cell contents. The stained chromosomes are also not monodisperse particles, as they can be divided into chromosome subtypes. Chromosome subtypes have a substantial difference in their dimension and shape, and their movement cannot be trivially compared with the $0.5\text{ }\mu\text{m}$ and

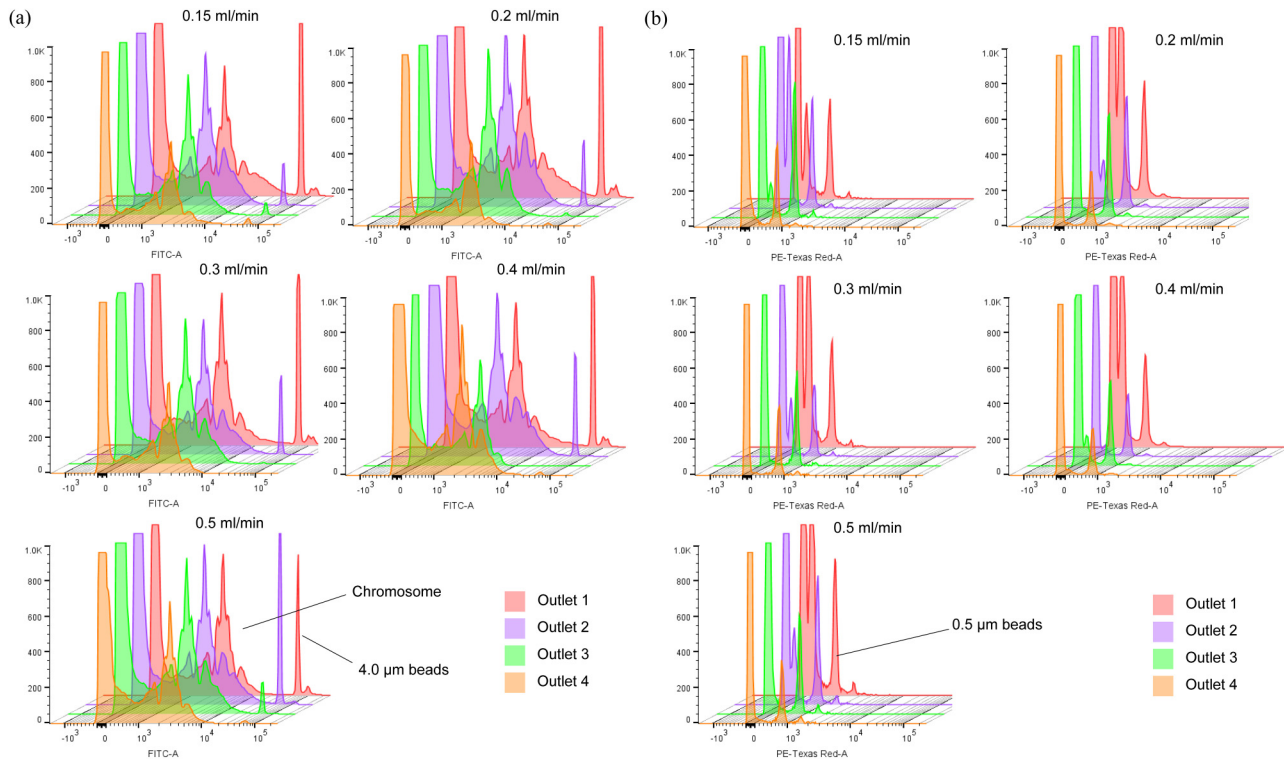


FIG. 4. FACS scan results of chromosome and bead distribution in the spiral channel outlets. (a) Distribution of the chromosome sample and $4.0\text{ }\mu\text{m}$ beads under different flow rates. (b) Distribution of $0.5\text{ }\mu\text{m}$ beads under different flow rates.

$4.0\text{ }\mu\text{m}$ beads due to this lack of uniform size and shape. As the chromosomes do not precisely follow beads' movement patterns, the influence of chromosome shape to chromosome focusing positions is substantial and deserves further analysis.

In a shear flow, the chromosomes have different rotational behaviors compared to spherical particles, which affects the chromosome inertial focusing process. The assumption that chromosomes become aligned in the spiral channel device helps explain chromosome focusing behavior under shear flow. It should be noted that the asymmetric chromosome particles experience a different distribution of Dean drag forces and inertial lift forces compared to spherical particles. When chromosomes become aligned with the fluid flow direction, F_L and F_D are calculated based on Eqs. (3) and (4) based on the chromosome front projection area A and aspect ratio γ . The dimensional chromosome subtype difference is analyzed as is shown in Fig. 6(a). In this case, the chromosomes are modeled as a rod-shaped particle. The particle projection area A is estimated by the area of the circular cross section. When the aspect ratio γ is close to 1, the shape of the chromosome is similar to a spherical fluorescent bead. When γ is high, the chromosome is a rod shape. Chromosome short axis and long axis are measured from the sorted chromosome image using the software ImageJ (version 1.53c, NIH), in which the image threshold is adjusted, and the chromosome dimension is acquired utilizing

the built-in analyze function. More than 30 samples are analyzed for chromosome subtypes, and the error bar indicates the variation of chromosome projection area and aspect ratio. For sister chromatids, the chromosome short axis a is the equivalent diameter of the circle with the same area of sister chromatids cross section. As a result, Fraction C has a smaller chromosome aspect ratio compared with Fraction B. Figure 6(a) shows that the chromosome projected area increases gradually in each fraction, which matches the fluorescent stain intensity during the FACS sorting process. The small condensed chromosome in Fraction A and nuclei found in Fraction D have a small aspect ratio, and their shapes are closer to the spherical beads. The single chromosomes, which form the main peak in the FACS intensity band, have the highest aspect ratio.

To quantify the influence of the inertial flow and the Dean flow on the chromosome movement, the lift and drag forces are estimated based on their shape difference. The magnitudes of F_L and F_D are calculated based on A and γ under different flow rates. The ratio of F_L and F_D , $M = F_L/F_D$ is proposed to characterize the chromosome fraction movement as is shown in Fig. 6(b). Table I shows the estimate of chromosome fraction movement due to A and γ . Fraction A has a low A and does not get focused in the inertial flow. As a result, F_D dominates the particle movement. Fraction B has a larger A , leading to an increase in F_L . However, Fraction B has the highest γ , and F_D dominated the particle movement.

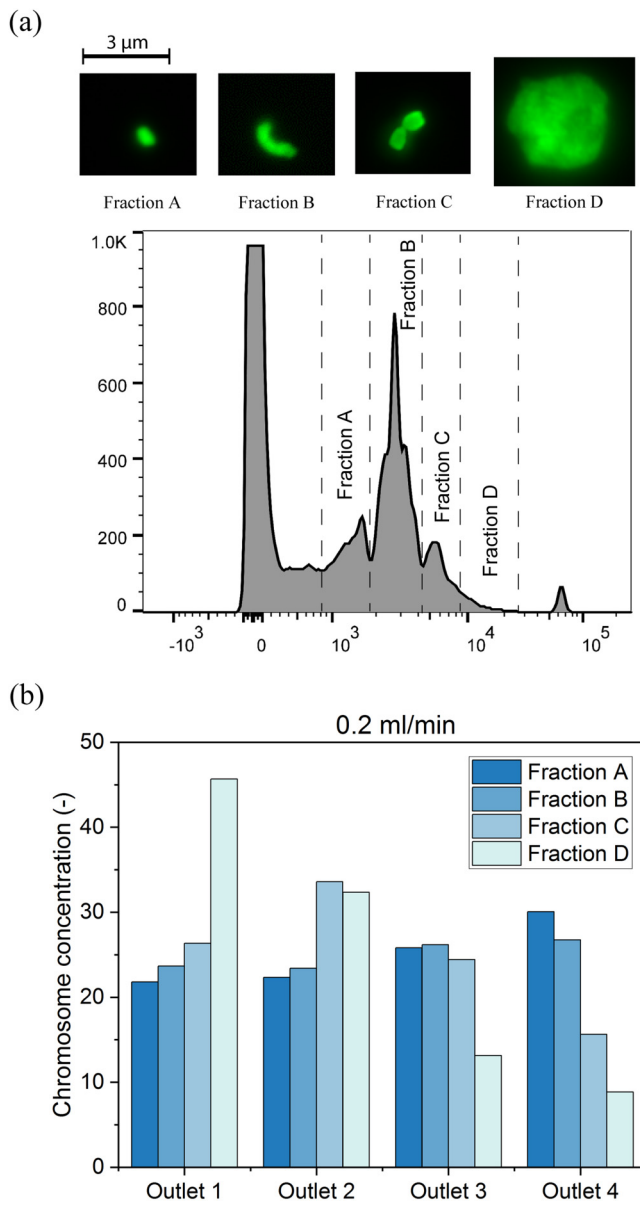


FIG. 5. (a) Representative images of sorted chromosome fractions from FACS. (b) Chromosome distribution in channel outlets at the flow rate of 0.2 ml/min.

Fraction A and Fraction B have a similar magnitude of M , which matches the observation that Fraction A and Fraction B have the same distribution in the spiral channel, as is shown in Figs. 5(b) and 6(c). Fraction C has medium A and γ , and it distributes to the middle of the channel. Fraction D has a high magnitude of A with a low γ , and F_L dominates the particle trajectory. As a result, for the capsule-shaped chromosome, M can be used to predict the particle movement and distribution in the spiral channel device.

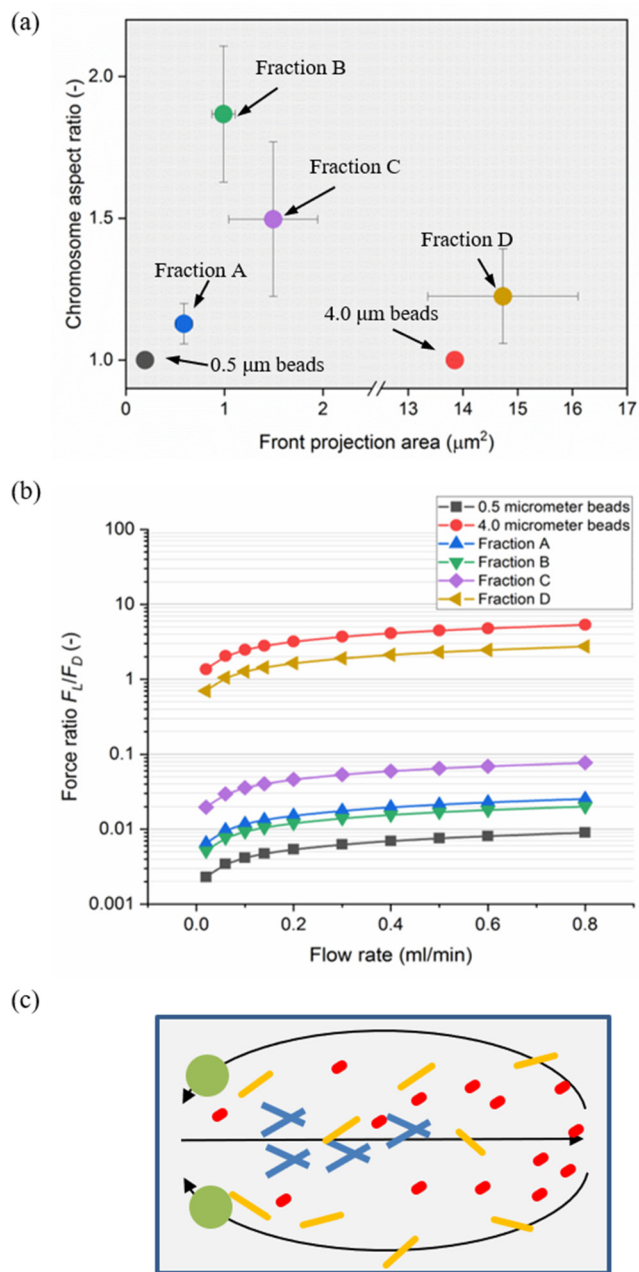


FIG. 6. (a) Projected area and aspect ratio of sorted fractions from FACS. (b) The ratio of shear lift force F_L to the Dean drag force F_D against the flow rate. (c) Proposed chromosome fraction distribution in the channel cross section.

The approach is verified by comparing the results in Figs. 4 and 5 with the predictions in Fig. 6.

Though the current results demonstrate the change of chromosome distribution in the device setup, the separation efficiency is still low as there is an overlap in the chromosome distribution

TABLE I. Influence of the particle projection area and the aspect ratio to force dominating particle trajectory.

	Fraction A	Fraction B	Fraction C	Fraction D
Projection area	Low	Medium	Medium	High
Aspect ratio	Low	High	Medium	Low
Dominated force	F_D	F_D	Balanced state	F_L

position. In Fig. 6(b), it is found that the Dean force is high for chromosome fraction A, B, and C. In the ideal case, the inertial force leads to particle focusing in narrow streams, and the Dean flow changes the particle focusing position. Improvement in the device design could lead to higher separation efficiency. For example, the shear lift force increases with the reduction of channel cross section dimension. Also, the channel aspect ratio, which is the ratio of channel width and channel height, affects the magnitude of the Dean flow. By adjusting the spiral channel design parameters, we could change the force distribution on the chromosome, leading to an improved separation resolution.

VI. CONCLUSION

In this research, experiments were performed to purify chromosomes from cell debris in a microfluidic spiral channel device. The spiral channel device is designed and fabricated for the separation of chromosomes using inertial focusing effects combined with the Dean flow drag force. Separation of chromosome particles from large $4.0\ \mu\text{m}$ beads was observed as chromosomes tend to focus toward the inner side of the channel. With the increase of the flow rate, the chromosomes have a different distribution compared to the fluorescent beads, and the FACS sorting results indicate that different types of chromosomes exist in the cell lysis sample, and the difference of chromosome size and shape leads to the change of chromosome focusing position in the spiral channel device, enabling chromosome enrichment and separation. For the more round-shaped chromosomes, their movement behavior is analogous to spherical particles with the commensurate size. High aspect ratio single chromosomes tend to be dispersed across the channel due to the increase of the Dean drag force, while groups of two chromosomes tend to have a higher shear lift force that leads to the particles focusing in the channel. The difference in chromosome projection area and aspect ratio for chromosome subtypes leads to the variation of the ratio of the shear lift force and the Dean drag force, leading to the change of chromosome exit position in the channel. Mathematical analysis demonstrated that the impact of aspect ratio led to the ability to predict the elution location of the particles. The current results indicate the possibility of separating groups of chromosomes based on their dimension and aspect ratio, which has the potential for creating a rapid chromosome karyotyping process. This separation principle can be applied for other bio-particles with a variety of shapes and aspect ratios.

SUPPLEMENTARY MATERIAL

See the [supplementary material](#) for the device design, results of the Dean flow fractionation sorting of fluorescent beads for

spiral channel device calibration, and the description of FACS elutes sorting process.

ACKNOWLEDGMENTS

This work was supported by the University of Utah Flow Cytometry Facility in addition to the National Cancer Institute through Award No. 5P30CA042014-24.

DATA AVAILABILITY

The data that support the findings of this study are available within the article and its [supplementary material](#) and are available from the corresponding author upon reasonable request.

REFERENCES

- ¹O. W. McBride and H. L. Ozer, “Transfer of genetic information by purified metaphase chromosomes,” *Proc. Natl. Acad. Sci. U. S. A.* **70**, 1258–1262 (1973).
- ²R. E. Fournier and F. H. Ruddle, “Microcell-mediated transfer of murine chromosomes into mouse, Chinese hamster, and human somatic cells,” *Proc. Natl. Acad. Sci. U. S. A.* **74**, 319–323 (1977).
- ³S. M. Gribble, F. K. Wiseman, S. Clayton, E. Prigmore, E. Langley, F. Yang *et al.*, “Massively parallel sequencing reveals the complex structure of an irradiated human chromosome on a mouse background in the Tc1 model of Down syndrome,” *PLoS One* **8**, e60482 (2013).
- ⁴A. O’Doherty, S. Ruf, C. Mulligan, V. Hildreth, M. L. Errington, S. Cooke *et al.*, “An aneuploid mouse strain carrying human chromosome 21 with Down syndrome phenotypes,” *Science* **309**, 2033–2037 (2005).
- ⁵H. Lodish, A. Berk, and S. Zipursky, “Section 9.6 morphology and functional elements of eukaryotic chromosomes,” in *Molecular Cell Biology*, 4th ed. (W. H. Freeman, New York, 2000).
- ⁶M. Yusuf, N. Parmar, G. K. Bhella, and I. K. Robinson, “A simple filtration technique for obtaining purified human chromosomes in suspension,” *BioTechniques* **56**, 257–261 (2014).
- ⁷J. G. Collard, E. Philippus, A. Tulp, R. V. Lebo, and J. W. Gray, “Separation and analysis of human chromosomes by combined velocity sedimentation and flow sorting applying single- and dual-laser flow cytometry,” *Cytometry* **5**, 9–19 (1984).
- ⁸N. Xiang and Z. Ni, “High-throughput blood cell focusing and plasma isolation using spiral inertial microfluidic devices,” *Biomed. Microdevices* **17**, 110 (2015).
- ⁹H. W. Hou, M. E. Warkiani, B. L. Khoo, Z. R. Li, R. A. Soo, D. S.-W. Tan *et al.*, “Isolation and retrieval of circulating tumor cells using centrifugal forces,” *Sci. Rep.* **3**, 1259 (2013).
- ¹⁰J. Son, K. Murphy, R. Samuel, B. K. Gale, D. T. Carrell, and J. M. Hotaling, “Non-motile sperm cell separation using a spiral channel,” *Anal. Methods* **7**, 8041–8047 (2015).
- ¹¹D. Carlo, J. F. Edd, K. J. Humphry, H. A. Stone, and M. Toner, “Particle segregation and dynamics in confined flows,” *Phys. Rev. Lett.* **102**, 094503 (2009).
- ¹²J. Zhou and I. Papapostky, “Fundamentals of inertial focusing in microchannels,” *Lab Chip* **13**, 1121–1132 (2013).
- ¹³D. Di Carlo, D. Irimia, R. G. Tompkins, and M. Toner, “Continuous inertial focusing, ordering, and separation of particles in microchannels,” *Proc. Natl. Acad. Sci. U. S. A.* **104**, 18892–18897 (2007).
- ¹⁴J. M. Martel and M. Toner, “Particle focusing in curved microfluidic channels,” *Sci. Rep.* **3**, 3340 (2013).
- ¹⁵J. M. Martel and M. Toner, “Inertial focusing dynamics in spiral microchannels,” *Phys. Fluids* **24**, 032001 (2012).
- ¹⁶J. Zhang, W. Li, M. Li, G. Alici, and N.-T. Nguyen, “Particle inertial focusing and its mechanism in a serpentine microchannel,” *Microfluidics Nanofluidics* **17**, 305–316 (2013).

- ¹⁷D. R. Gossett and D. Carlo, "Particle focusing mechanisms in curving confined flows," *Anal. Chem.* **81**, 8459–8465 (2009).
- ¹⁸A. Russom, A. K. Gupta, S. Nagrath, and D. D. Carlo, "Differential inertial focusing of particles in curved low-aspect-ratio microchannels," *New J. Phys.* **11**, 75025 (2009).
- ¹⁹S. S. Kuntaegowdanahalli, A. A. Bhagat, G. Kumar, and I. Papautsky, "Inertial microfluidics for continuous particle separation in spiral microchannels," *Lab Chip* **9**, 2973–2980 (2009).
- ²⁰A. S. Bhagat, S. S. Kuntaegowdanahalli, and I. Papautsky, "Continuous particle separation in spiral microchannels using Dean flows and differential migration," *Lab Chip* **8**, 1906–1914 (2008).
- ²¹D. Qi and L. Luo, "Transitions in rotations of a non-spherical particle in a three-dimensional moderate Reynolds number Couette flow," *Phys. Fluids* **14**, 4440–4443 (2002).
- ²²M. Masaeli, E. Sollier, H. Amini, W. Mao, and K. Camacho, "Continuous inertial focusing and separation of particles by shape," *Phys. Rev. X* **2**, 031017 (2012).
- ²³M. Trebbin, D. Steinhauser, J. Perlich, A. Buffet, S. V. Roth, W. Zimmermann *et al.*, "Anisotropic particles align perpendicular to the flow direction in narrow microchannels," *Proc. Natl. Acad. Sci. U. S. A.* **110**, 6706–6711 (2013).
- ²⁴C. Prohm, N. Zöller, and H. Stark, "Controlling inertial focussing using rotational motion," *Eur. Phys. J. E* **37**, 36 (2014).
- ²⁵W. E. Uspal, H. B. Eral, and P. S. Doyle, "Engineering particle trajectories in microfluidic flows using particle shape," *Nat. Commun.* **4**, 2666 (2013).
- ²⁶D. Leith, "Drag on non-spherical objects," *Aerosol Sci. Technol.* **6**, 153–161 (1987).
- ²⁷H. Feng, M. Hockin, S. Zhang, M. Capecchi, B. Gale, and H. Sant, "Enhanced chromosome extraction from cells using a pinched flow microfluidic device," *Biomed. Microdevices* **22**, 25 (2020).